JOURNAL OF GEOPHYSICAL RESEARCH, VOL. 104, NO. B6, PAGES 12,779–12,796, JUNE 10, 1999

Investigation of the relationships between basin morphology, tectonic uplift, and denudation from the study of an active fold belt in the Siwalik Hills, central Nepal

J.-E. Hurtrez[1] and F. Lucazeau[2]

Laboratoire de Géophysique et Tectonique, UMR 5573 CNRS Université de Montpellier II, Montpellier, France

J. Lavé

Laboratoire de Géodynamique des Chaînes Alpines, Université Joseph Fourier, Grenoble, France

J.-P. Avouac

Laboratoire de Géophysique, CEA, Bruyères-le-Châtel, France

Abstract. The present study investigates correlations between an extensive range of geomorphic properties that can be estimated from a digital elevation model and the uplift rate on geological timescales. The analysis focuses on an area in the Siwalik Hills (central Nepal), where lithology and climate can be considered as uniform. This area undergoes rapid tectonic uplift at rates of up to 15 mm yr^{-1}, which are derived from the geometric pattern of a fault-bend model of fold growth. The selected geomorphic properties can be divided in two categories, depending on whether or not the vertical dimension is taken into account. None of the planar properties are significantly correlated to uplift rate, unlike those that include the vertical dimension, such as the mean elevation of basins, hypsometric curve, and hypsometric integral, and relief defined by the amplitude factor of length scaling analysis. Correlation between relief and uplift rate is observed for all length scales of topography shorter than 600 m, which suggests that all orders of the streams are able to adjust to the tectonic signal. Simple mass balance considerations imply that the average elevation is only 10% of surface uplift, suggesting that a dynamic equilibrium has been reached quite rapidly. Using a simple two-process model for erosion, we find that fairly high diffusion coefficients (order of 10 m^2 yr^{-1}) and efficient transport of the material by rivers are required. This unusually high value for mass diffusivity at small length scales may be obtained by either a very efficient linear diffusion or by landsliding. Actually, both processes may be active, which appears likely given the nature of the unconsolidated substratum and the favorable climatic conditions. Local relief in the study area may therefore be used to predict either uplift or denudation, but the prediction is calibrated only for that specific climatic and lithologic conditions and cannot be systematically applied to other contexts.

1. Introduction

As a whole, a landscape results from the competition of tectonic and geomorphic processes (e.g., denudation of hillslopes, sedimentation, and river incision). Various authors have shown therefore that some information on the rate of tectonic processes may be retrieved from a geomorphological approach. For example, the geometry of marine terraces [e.g., *Lajoie*, 1986; *Armijo et al.*, 1996] or of fluvial terraces [e.g., *Rockwell et al.*, 1984; *Bull and Knuepfer*, 1987; *Merritts et al.*, 1994] may be used to derive rates of tectonic uplift or river incision. This kind of approach is focused on specific geomorphic features that can be assigned an age and an initial geometry. One the other hand, several authors have explored whether information could also be retrieved from the global analysis of landscape topography [e.g., *Ahnert*, 1970, 1984; *Koons*, 1989; *Ohmori*, 1993]. The topography is one characteristic of a landscape that may appear incomplete in view of the complexity of the various interacting processes that produce it. However, it is easily accessible and particularly amenable to quantification, especially when digital elevation models (DEMs) are used. The dependence of topography on forcing factors has therefore attracted much attention, in the hope that tectonic input or intensity of erosional processes may be retrieved from simple geometric properties of the landscape. In some cases, some geomorphic indices have actually been related successfully to tectonics [*Mayer*, 1986; *Merritts and Vincent*, 1989; *Willemin and Knuepfer*, 1994] or to denudation [*Ahnert*, 1970, 1984]. The difficulty in such case studies is generally that the forcing factors (tectonic uplift, eustatic sea level changes, and

[1]Now at Laboratoire de Géologie, UMR 8538 CNRS Ecole Normale Supérieure, Paris.
[2]Also at ELF Aquitaine, Pau, France.

Paper number 1998JB900098.
0148-0227/99/1998JB90009$9.00

paleoclimatic conditions) are poorly constrained or vary simultaneously. The problem has therefore also been tackled using numerical modeling [*Koons*, 1989; *Chase*, 1992; *Lifton and Chase*, 1992; *Willgoose*, 1994]. This latter approach identifies the specific contribution of a given parameter to the landscape properties through parametric studies but suffers from our poor understanding of surface processes, which can be constrained mainly by approaches of the first type. It is therefore important to find a case study where factors of control are well constrained and vary independently of each other.

In this paper we examine the morphologic properties of a natural landscape, for which the various forcing factors are constrained with some accuracy and where variations of tectonic uplift are apparently dominant over lithologic and climatic variations. The study area lies in the Siwalik Hills of central Nepal. Analysis is focused on the frontal hill range that consists of relatively homogeneously distributed conglomerates, mudstones and sandstones and that experiences particularly rapid uplift, up to 1.5 cm yr^{-1}, with respect to the Ganges basin that controls the local base level (J. Lavé and J.-P. Avouac, Active folding of fluvial terraces across the Siwalik Hills, Nepal, submitted to *Journal of Geophysical Research*, hereinafter referred to as Lavé and Avouac). A possible aspect of this landscape is that denudation could balance tectonic uplift (Lavé and Avouac) because of the exceptional efficiency of denudation. This is therefore an unique opportunity to investigate whether or not an analysis of a DEM can provide a quantitative information on these relationships between tectonic uplift and denudation.

In section 2 we review some geomorphic indices that best characterize landscapes and that have been previously shown to be sensitive to controlling factors in morphogenesis. In sections 3 and 4 we describe the study area and search for the significant correlations between uplift rate and morphometric indices. In section 5 we investigate the possibility that this landscape is in dynamic equilibrium on the basis of numerical simulations. In section 6 we discuss the possibility for predicting uplift rate from the morphologic properties of DEMs.

2. Review of Drainage Basins Morphometry and Influence of Forcing Factors

A drainage basin, or watershed, consists of two interrelated subsystems: the channel network and the hillslopes. Hereafter, we review geomorphic indices related to each subsystem, representative either of their planar geometry or their three-dimensional (3-D) geometry. Definitions and mathematics of these indices are given in the appendix.

2.1. Channel Network

Given that the channel network is the main agent of transport for the material eroded away from a drainage basin, one may expect that its characteristics are correlated with denudation rates and/or uplift rates. Several experimental or case studies have evidenced successfully such a relationship with channel network characteristics: (1) drainage density (from flume experiments [*Mosley*, 1972] and from numerical simulations [*Rinaldo et al.*, 1995], (2) geometry of the main stream (or trunk stream), especially the stream gradient (from flume experiments [*Begin et al.*, 1981], hydrological considerations [*Schumm*, 1986], numerical simulations [*Mizutani*, 1996], and case studies of natural examples [*Seeber et al.*, 1981; *Keller*, 1986; *Merritts and Vincent*, 1989; Lavé and Avouac]).

Many authors have pointed out that the response of the drainage network to forcing factors, including uplift, may actually be scale dependent [e.g., *Merritts and Vincent*, 1989]. This requires to take into account the hierarchical organization of the drainage network by the ordering technique proposed by *Strahler* [1952a] or the geometric properties integrated over a wide range of scale such as the coefficients and exponents of fractal laws. For example, in their study of coastal basins in the Mendocino Triple Junction region (California), *Merritts and Vincent* [1989] observed that the lower-order streams are more sensitive to uplift rate in terms of their gradient, length, area, and drainage density. On the other hand, scaling relationships theoretically can allow the detection of such thresholds and influence of the controlling factors. The stream gradient generally obeys a scaling law that relates the average slope to a given point within a reach to the drainage area [*Willgoose*, 1994] (hereafter referred to as Flint's law, see the appendix). The two parameters of this law, β and C_s, thus provide a convenient characterization of the gradient of the main stream accounting for its scale dependence. However, theoretical considerations show that the uplift rate should be correlated with coefficient C_S of Flint's law but not with the exponent β [*Willgoose*, 1994].

2.2. Drainage Basin

2.2.1. Basin shape. Some of the geometric characteristics in plan view of a drainage basin have been related to the tectonic input, such as aspect ratio, axial ratio and quartile width ratio [*Mayer*, 1986; *Willemin and Knuepfer*, 1994; *Hovius*, 1996] (See the appendix for definitions). However, drainage basin shape may be also controlled by the nature of mountain ranges [*Mayer*, 1986], as suggested by the linear relationship between spacing of basin outlets and the width of the range [*Hovius*, 1996]. For a large-scale analysis, both measurements on natural basins [*Hovius*, 1996] and theoretical results [*Deschaux and Souriau*, 1996] suggest a constant basin aspect ratio. However, at a smaller scale the basin axial ratio has been shown to vary in different geomorphic domains, depending on their tectonic history [*Willemin and Knuepfer*, 1994].

2.2.2. Hypsometry. The hypsometric curve and integral [*Strahler*, 1952b] quantify the distribution of elevations within a basin (see the appendix). Initially, these variables were defined to characterize the stage of geomorphic development [*Strahler*, 1952b; *Ohmori*, 1993]. It has been shown later on the basis of numerical modeling and observations on drainage basins in Japan [*Ohmori*, 1993] that they may actually be representative of the intensity of erosion. Hypsometry may be correlated therefore with tectonic uplift providing that basins with similar geomorphic maturity are compared [*Lifton and Chase*, 1992; *Ohmori*, 1993].

2.2.3. Relief. Relief refers to a difference in elevation at a given horizontal scale [*Summerfield*, 1991]. It represents a fundamental attribute widely recognized to reflect the interplay between tectonics and erosion. The relief may be quantified in various ways. "Basin relief" generally refers to the difference in elevation between the highest and lowest

points in the basin. This quantity can be scaled according to the size of the basin and becomes the "relief ratio" within the basin (see the appendix). The local relief, as first introduced by *Ahnert* [1970], provides some measure of the roughness of the topography within the basin. It is defined as the average difference in elevation within a sliding window of a given size [see also *Summerfield*, 1991] (the appendix). Relief can also be considered as a measure of the surface roughness (expressed as the fractal dimension of the topography). From numerical simulations of landscape evolution, relief has been shown to be primarily controlled by climate and uplift rate [*Chase*, 1992; *Rinaldo et al.*, 1995]. However, at small scales in southern Arizona, rock type and geologic structures are the dominant factors in controlling relief variations [*Chase*, 1992].

One problem of this definition of relief is that it is scale dependent and that depending on the scale, it may relate to different morphological characteristics. It has been observed that the local relief follows some power law function of the length scale, λ (see the appendix) [e.g., *Weissel et al.* 1994]. The exponent of the power law (Hurst exponent) is relatively insensitive to forcing factor [*Weissel et al.*, 1994]. Thus the amplitude factor (Cr) provides a convenient measure of the relief accounting for various length scales and should be most sensitive to forcing factors [*Weissel et al.*, 1994]. When local relief is expressed as a function of length scale, three different domains are generally observed [*Vergne and Souriau*, 1993; *Lucazeau and Hurtrez*, 1997]. The microscale relief (λ<~100 m) increases linearly with the length scale (H_1~1) and would be controlled by diffusive-like processes on hillslopes. The mesoscale relief is some power law function of the length scale (H_2~0.5) that would be controlled by fluvial processes [*Willgoose*, 1994; *Lucazeau and Hurtrez*, 1997]. At the large scale (macroscale) the relationship is again linear (H_3~1) [*Vergne and Souriau*, 1993; *Lucazeau and Hurtrez*, 1997]. To characterize the topographic roughness within a basin, one may thus either use relief at selected length scales or the value of the Hurst parameters at the micro, meso, or macroscale.

This review shows that some morphometric properties of a landscape may be representative of tectonic uplift and denudation rate, but most case studies are ambiguous due to the uncertainty on the controlling factors. Furthermore, characteristics of drainage basins can result from the effect of different forcing factors as well as self-organization processes. Thus, in order to decipher the geomorphological impact of tectonics, and its relationship with erosion, it is crucial to select a study area where the forcing factors in landscape building are well constrained and where the variations of the uplift and denudation rates dominate the variation of other parameters.

3. Characteristics of the Study Area

3.1. Geographic and Climatic Setting

The selected area is located 60 km to the southeast of Kathmandu (Nepal), between the Bakeya and the Bagmati rivers. It covers a zone of 790 km^2 (Figures 1a and 1b) within the Siwalik Hills which form an east-west trending low-elevation fold belt. The Siwalik Hills reach elevations about 920 m above the Ganges basin, which lies at an elevation of about 200 m on average (Figure 1a).

The Siwalik Hills are affected by an extremely humid and hot monsoonal climate that can be considered to be uniform at the scale of investigation. Annual mean temperature is of the order of 22°C. About 70% of the >2000 mm yr^{-1} annual precipitation falls within 3 months. A high erosional regime is induced with intense chemical weathering, sustained mass wasting on hillslopes, and efficient fluvial transport along stream channels.

3.2. Lithology

The bedrock consists of Tertiary molasse that have been eroded from the Himalaya and accumulated over the Indian basement since the middle Miocene [e.g., *Medlicot*, 1964; *Apple et al.*, 1991; *Harrison et al.*, 1993]. Three lithostratigraphic units are generally distinguished: the Lower, the Middle, and the Upper Siwaliks (Figures 1a and 1b). The Lower and Middle Siwaliks consist of fine-grained sandstones and mudstones with an increasing proportion of massive sandstones in the Middle Siwaliks. There is no clear morphologic contrast between the two units (Figure 1a). On the other hand, the Upper Siwaliks mainly consist of loose dark conglomerates that give rise to a different landscape (Figure 1a). The Upper Siwaliks are characterized by highly eroded landscape with low elevation and low relief. In the study area the summit of the hills is defined by massive Middle Siwalik sandstones.

3.3. Tectonics

The Siwalik units are presently being thrust over the recent alluvial sediments of the Ganges foreland basin, along the Main Frontal Thrust (MFT), which is the southernmost exposed thrust fault of the himalayan orogen. The Siwalik units have been deformed by thin-skinned tectonics induced by underthrusting of the Indian basement beneath the Lesser Himalaya [*Delcaillau et al.*, 1987]. The Siwalik Hills correspond to the topographic expression of the Main Frontal Thrust fault that is assumed to reach the surface along the southern limb of the fold belt [*Nakata*, 1989]. As shown in far eastern Nepal [*Schelling and Arita*, 1991], structural sections across the study area reveal a simple anticline structure (fault-bend fold) related to a 25-50° northward dipping ramp, rooting into a horizontal décollement at the base of the 5-6 km thick Siwalik group (inset in Figure 1b) (Lavé and Avouac). The shallowing of Siwalik units dips away from the MFT probably reflects the flattening of the underlying MFT and indicate a listric shape for the thrust fault [*Schelling and Arita*, 1991].

3.4. Distribution of Active Uplift

A correlation between structural geology (bedding dips) and uplift is predicted by the fault-bend fold model [*Suppe*, 1983]. In order to test if the fault-bend fold model is valid in the study area, numerous fluvial terraces were observed and studied along two major rivers that cut across the fold belt, the Bagmati and the Bakeya (Lavé and Avouac). In order to deduce the tectonic deformation, from abandoned terraces profiles, a good control on their geometry was needed. It was obtained from a detailed mapping and elevation measurements in the field and from a high resolution DEM. The initial geometry of the terraces was also needed. Therefore a particular attention was paid to strath terraces because they are beveled into the valley-wall bedrock and are

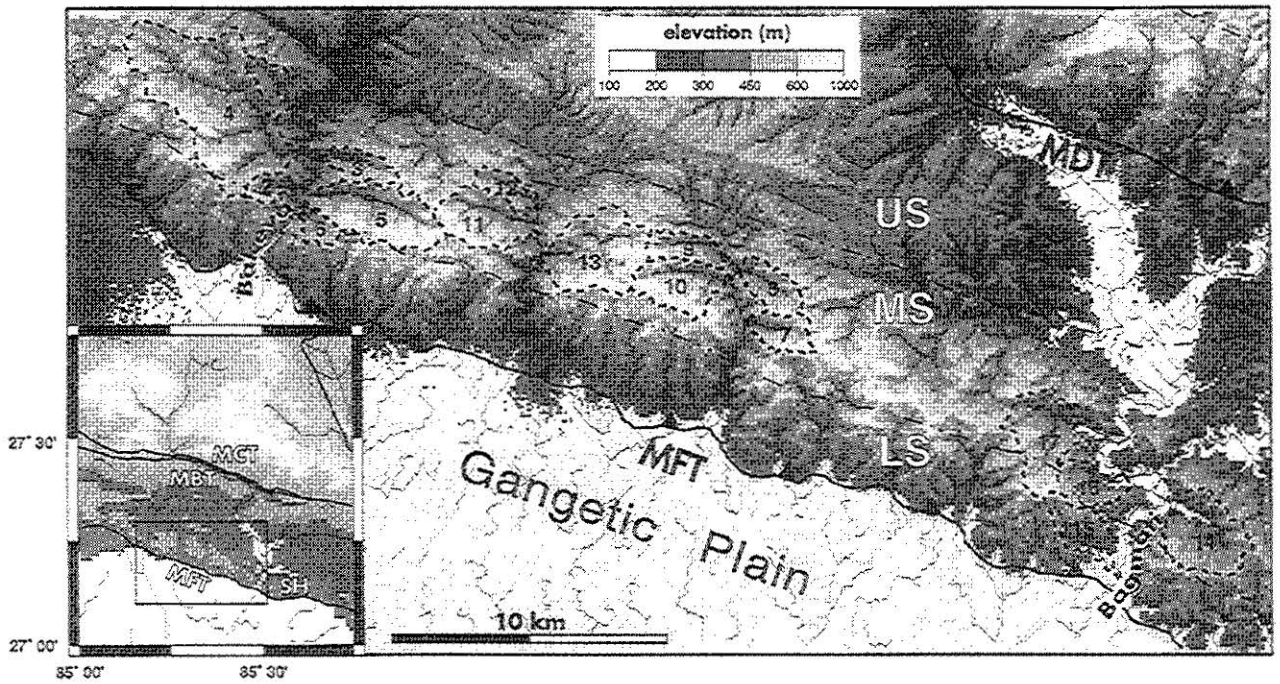

Figure 1a. Topographic map of the study area in the Siwalik Hills; thin solid lines represent the river networks extracted from the DEM. For clarity, the threshold used for channel extraction is about 1 km^2 (greater than the 3.84×10^{-2} km^2 used in the text for the characterization of geomorphic parameters). Thick dashed lines delineate the drainage basins used for geomorphic analyses. Dashed-dotted lines delineate the lithologic units: LS, Lower Siwaliks; MS, Middle Siwaliks; US, Upper Siwaliks; MFT, Main Frontal Thrust; MDT, Main Dun Thrust. Inset map shows the location of the study area (box) 60 km south east of Kathmandu; MCT, Main Central Thrust; MBT, Main Boundary Thrust; MFT, Main Frontal Thrust; SH, Siwalik Hills.

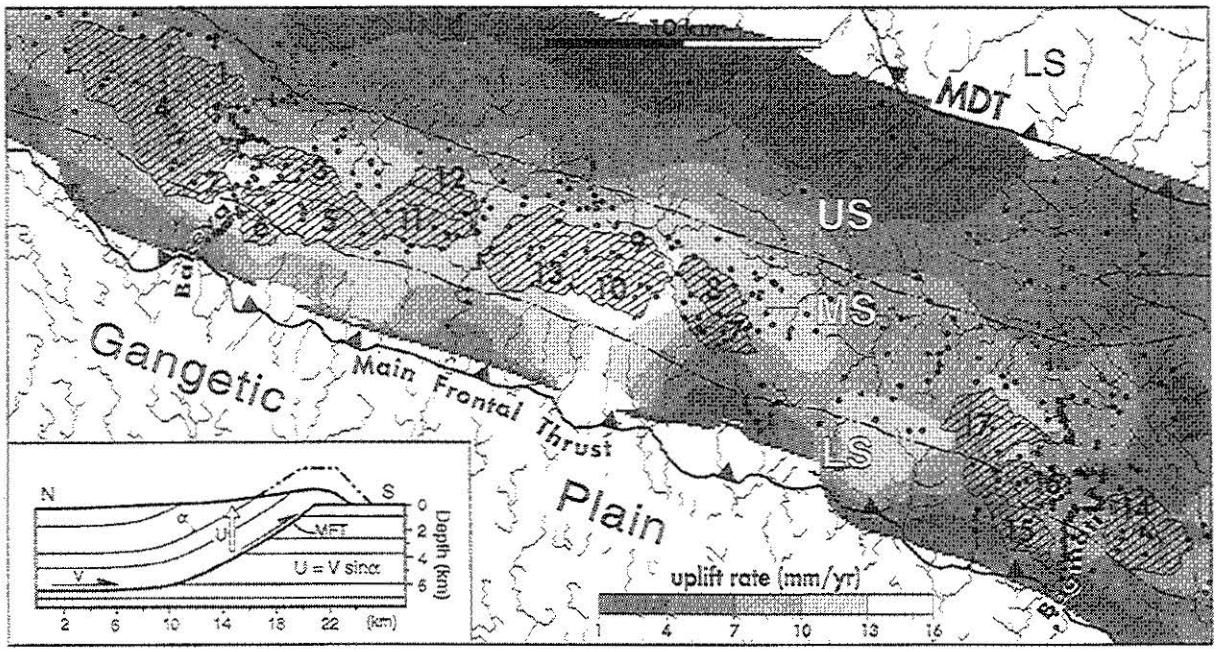

Figure 1b. Simplified structural map of the study area. The sub-Himalaya is thrust over recent alluvial sediments of the Ganges basin along the Main Frontal Thrust. Inset map shows a schematic section across the Siwalik Hills illustrating the fault-bend folding geometry and the method used to infer the uplift rate (U) from the dip of the beds (α, assumed parallel to the dip of the ramp) and convergence rate (V=21 mm yr^{-1}). Uplift rate (mm yr^{-1}) is depicted by the gray scale and ranges from 2 to 16 mm yr^{-1}. Dots indicate location of the bedding dips measurements used to estimate the uplift rate. Dashed-dotted lines delineate the lithologic units: LS, Lower Siwaliks; MS, Middle Siwaliks; US, Upper Siwaliks; MDT, Main Dun Thrust; MFT, Main Frontal Thrust.

supposed to form along reaches at equilibrium [*Bull*, 1991; *Merritts et al.*, 1994]. In the field, four major levels of strath terraces were recognized and were surveyed along the Bagmati and Bakeya rivers. Radiometric ages of charcoals found in six different sites along the Bagmati and Bakeya rivers attested that these terraces were formed during Holocene (2-10 kyr) (Lavé and Avouac). Because straths form when the stream has excess power for meander migration and lateral bank erosion [*Merritts et al.*, 1994], the terraces were probably formed during wet climatic conditions. The abandonment of strath terraces occurred at wet-to-dry climatic transitions in the Holocene period as evidenced by the correlation between the radiometric age of the veneer of deposits on strath terraces and wet to dry climatic transitions recorded in Tibetan lakes (Lavé and Avouac).

Qualitatively, the profiles of the four levels of strath terraces along the Bakeya and the Bagmati rivers were in agreement with an active growth of the MFT fold during the Holocene. This exceptional record of river incision in the study area was used to demonstrate quantitatively the validity of the fault-bend fold model for the fold belt growth (Lavé and Avouac). According to such a kinematic model the tectonic rock uplift, U, at any point should be proportional to the horizontal shortening rate across the fold, V:

$$U = V \sin(\alpha) \quad (1)$$

where α is the dip of the beds assuming parallelism with the dip of the ramp.

Uplift profiles of terrace levels surveyed along the Bagmati and Bakeya rivers were found in good agreement with the bedding dips as predicted by (1). A shortening rate of 21 ± 1.5 mm yr^{-1} (at the 1σ confidence level), consistent with the four levels of folded fluvial terraces, was deduced (Lavé and Avouac). According to the fault-bend fold model the hanging wall accommodates the deformation imposed by the flat to ramp bend by bedding slip without any change in length and width of the beds, which is consistent with field observations (Lavé and Avouac). Frequent mudstone and claystone layers accommodate bedding slip between more competent and thicker sandstone layers.

Once validated, and according to the cylindrical geometry of the structures in the study area, the tectonic model was used to derive tectonic uplift at all points where bedding dips had been measured in the field. Additional dip measurements were derived from the DEM, in the Middle Siwaliks, where massive sandstones with structural slope dipping NNW define the crest of the hills (Lavé and Avouac) (Figure 1b). The map shown in Figure 1b was derived by interpolating this data set [*Lavé*, 1997]. The interpolation smoothed out the local variations of uplift rates related to the local variations of bedding dips. Therefore uplift rates variations are significant for length scales longer than 100 m. In the study area the estimated uplift rates are exceptionally high and range from 2 to 16 mm yr^{-1} (Figure 1b).

In the tectonic model the isostatic contribution to the uplift is neglected. Indeed, according to the flexural rigidity of the Indian lithosphere ($D \sim 7.10^{24}$ N m), inferred from gravity anomalies and topographic characteristics in the Ganges basin [*Lyon-Caen and Molnar*, 1983], the flexure of the lithosphere can only develop large wavelength deformation of about 1000 km. Therefore, the wavelengths ranging from 1 to 10 km, which we are considering here, have negligible effects.

4. Data and Methods

4.1. Characteristics of the DEM

The DEM consists of a grid of elevations derived from a pair of stereoscopic SPOT satellite images. It is expressed in a universal transverse Mercator (zone 45) projection. The node spacing is 20 m. Elevations were calculated by a cross-correlation method within a sliding window and can be considered accurate to better than 15 m. This technique leads to the smoothing of the topography at short length scales [*Weissel et al.*, 1994].

The power spectrum (Figure 2) is typical of a self-similar topography for wavelengths greater than 200 m since it approximately follows a power law [*Turcotte*, 1992]. The rugosity of the DEM is approximately a white noise at wavelengths less than 50 m (flat power spectrum; Figure 2). This suggests that the topography is probably not correctly resolved at these short wavelengths. In the following, we will therefore only consider the characteristics of the topography at length scales greater than 200 m.

4.2. Extraction of the Channel Network and Drainage Basins

In order to extract the river networks from the DEM, the software "MAD" [*Moussa et al.*, 1997] was used. This software is based on the standard methods described by *Band*

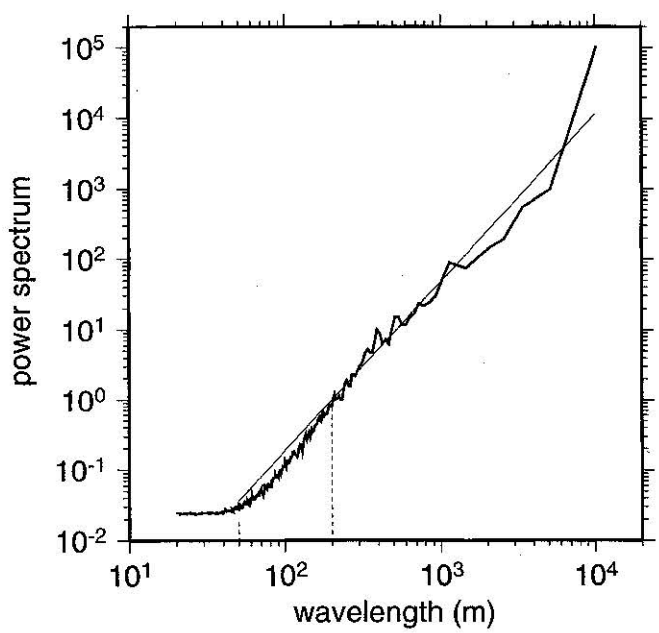

Figure 2. Power spectrum of north-south topographic profiles across the study area, calculated from the fast Fourier transform algorithm [*Press et al.*, 1989] (thick line). The power law relationship for wavelengths above 200 m suggests a self-similar topography (light solid line) [*Turcotte, 1992*]. At wavelengths between 50 and 200 m, the power spectrum is depressed compared to that of a self-similar topography. At wavelengths shorter than 50 m the flat power spectrum is typical of random noise. Thin solid line is the power law estimated by least squares adjustment; power spectrum is $3.14\ 10^{-6}\ \lambda^{2.40}$.

Table 1. Geomorphic Characteristics of Channel Networks and Drainage Basins

			Hack's Law		Flint's Law		
	Basin Area, km^2	Drainage Density, $km\ km^{-2}$	α	C_l	β	C_s	Uplift Rate, $mm\ yr^{-1}$
1	2.77	3.49	0.624	1650.78	-0.416	148.69	8.81
2	1.26	3.49	0.656	1585.44	-0.284	224.19	14.95
3	2.56	3.32	0.610	1713.60	-0.256	167.28	12.19
4	20.13	3.28	0.645	1360.97	-0.369	107.95	9.61
5	8.35	3.12	0.626	1443.81	-0.352	236.35	13.08
6	1.37	3.54	0.652	1452.91	-0.271	198.87	13.47
7	2.68	3.00	0.545	1461.23	-0.217	186.36	8.51
8	2.96	2.96	0.652	1390.66	-0.371	168.47	11.19
9	2.55	3.14	0.634	1772.56	-0.358	170.98	14.37
10	5.05	3.19	0.625	1472.52	-0.288	209.80	14.41
11	5.73	3.12	0.624	1440.95	-0.201	135.70	11.67
12	2.03	3.11	0.890	1631.44	-0.415	95.28	10.94
13	8.72	3.15	0.574	1583.11	-0.207	143.02	13.16
14	7.21	2.97	0.476	1541.10	-0.194	163.69	7.87
15	3.64	2.94	0.720	1608.64	-0.429	184.77	6.41
16	3.26	3.36	0.533	1826.92	-0.274	197.88	8.57
17	7.41	3.00	0.638	1404.11	-0.214	164.93	9.54

	First Order				Second Order				Third Order			
	Number of Segments	Length, m	Area, km^2	Gradient, $m\ km^{-1}$	Number of Segments	Length, m	Area, km^2	Gradient, $m\ km^{-1}$	Number of Segments	Length, m	Area, km^2	Gradient $m\ km^{-1}$
1	17	265.2	0.095	176.8	5	641.6	0.410	129.9	2	654.2	1.01	28.6
2	9	298.1	0.099	307.5	2	373.8	0.283	201.2	1	947.7	1.26	162.5
3	19	263.3	0.089	234.8	3	758.3	0.685	281.5	1	1220.8	2.56	58.1
4	137	246.2	0.091	221.1	32	451.1	0.349	176.8	6	1594.2	2.22	80.5
5	62	189.4	0.083	324.8	11	759.4	0.465	253.9	1	5961.6	8.34	52.5
6	11	285.4	0.091	266.8	2	534.6	0.421	222.4	1	627.7	1.34	226.2
7	20	227.0	0.094	285.3	3	544.5	0.375	205.7	1	1860.2	2.68	103.8
8	22	211.4	0.103	202.8	5	470.3	0.412	221.3	1	1767.1	2.96	47.0
9	21	178.7	0.073	260.9	5	378.4	0.264	211.0	1	2343.1	2.53	47.8
10	36	206.4	0.085	309.3	8	653.0	0.426	234.4	2	420.4	0.90	202.2
11	37	236.2	0.100	243.1	8	595.7	0.410	191.4	2	1233.7	1.94	85.4
12	15	221.2	0.081	204.2	3	437.3	0.366	56.1	1	1685.1	2.02	52.2
13	64	223.4	0.090	257.1	12	562.4	0.430	205.8	3	1121.3	1.62	107.8
14	50	197.2	0.092	256.2	11	620.7	0.444	233.7	2	1465.1	2.50	103.9
15	22	200.0	0.101	249.6	5	555.2	0.436	130.6	2	637.7	1.18	86.2
16	24	201.2	0.080	255.0	6	491.2	0.296	226.6	3	567.7	0.81	101.5
17	51	213.5	0.090	256.4	14	282.3	0.248	221.6	4	720.1	0.98	155.1

[1986]. A single flow drainage direction following the steepest downward slope is calculated for each cell of the mesh. Sinks are filled, given a user supplied threshold area, to ensure the continuity of drainage. The channel network is extracted according to a constant threshold contributing area of 96 cells, or $3.84\times10^{-2}\ km^2$, arbitrarily chosen within the range proposed by *Montgomery and Dietrich* [1989]. A drainage basin is defined as the set of cells related to the basin outlet by their flow pathway.

4.3. Characteristics of the Selected Basins

We selected 17 basins, exposed to different uplift rates, in order to highlight the dependence of drainage basin morphology on tectonic uplift. The basins were chosen in areas with a high density of bedding dip measurements so that uplift rates could be well constrained from the fault-bend fold model (Figure 1b). Their areas range from 1.26 to 20.1 km^2 (Table 1). The zonal average uplift rate within each selected basin was computed from the interpolated function shown in Figure 1b. They range between 6.4 and 15.0 $mm\ yr^{-1}$ (Table 1). Climatic conditions can be considered as uniform over the study area. The basins are all located over the Lower or Middle Siwalik formations (Figures 1a and 1b) so that the influence of lithology on the variability of basin morphology is probably negligible. The main factor that should induce some variability in the morphometric properties of these basins is therefore the wide range of tectonic uplift rates.

Table 1. (continued)

	Axial Ratio	Mean Elevation, m	Local Base Level, m	Hypsometric integral	Basin Relief,m	Relief Ratio	Local Relief						Uplift Rate, mm yr^{-1}
							Cr_1	H_1	t_1, m	Cr_2	H_2	t_2, m	
1	0.619	366.8	232	0.371	366	0.153	0.227	0.997	104	1.508	0.590	1017	8.81
2	0.562	470.2	205	0.564	449	0.266	0.294	1.065	90	1.909	0.640	913	14.95
3	0.389	475.7	217	0.512	488	0.169	0.278	1.024	107	2.259	0.572	1399	12.19
4	0.489	478.9	220	0.462	565	0.078	0.179	1.101	107	1.751	0.599	2280	9.61
5	0.404	555.3	210	0.486	707	0.138	0.250	1.104	96	2.561	0.592	2184	13.08
6	0.701	496.8	203	0.577	523	0.332	0.234	1.055	90	0.704	0.791	916	13.47
7	0.584	581.1	280	0.567	489	0.202	0.274	1.029	102	2.063	0.607	1264	8.51
8	0.483	525.0	322	0.453	442	0.158	0.402	0.937	133	2.276	0.580	1017	11.19
9	0.355	536.2	334	0.423	471	0.156	0.322	0.999	104	2.774	0.541	1318	14.37
10	0.581	618.7	310	0.492	575	0.173	0.321	1.023	88	2.097	0.608	2210	14.41
11	0.578	550.5	303	0.427	579	0.163	0.329	0.998	96	1.916	0.612	2299	11.67
12	0.342	481.6	315	0.488	339	0.123	0.263	1.004	102	3.745	0.442	1624	10.94
13	0.771	584.5	282	0.484	611	0.161	0.217	1.106	92	2.240	0.588	3427	13.16
14	0.784	385.3	135	0.473	508	0.149	0.234	1.034	97	1.111	0.691	3013	7.87
15	0.419	331.9	125	0.341	616	0.185	0.232	1.033	113	1.445	0.644	1255	6.41
16	0.589	388.8	143	0.420	600	0.226	0.245	1.018	104	0.810	0.757	1715	8.57
17	0.814	432.2	150	0.480	588	0.173	0.195	1.105	94	1.722	0.624	1570	9.54

The regional base level, defined by the elevation of the Indian plain south of the fold belt, varies from about 120 m near the Bagmati to about 170 m near the Bakeya. The outlets of these basins are controlled by the four major rivers cutting across the anticline: the Bagmati, the Bakeya, and two intervening smaller rivers. The corresponding local base levels, defined as the elevation at the outlet of each basin, range from 125 to 334 m (Table 1). The drainage density is relatively constant and ranges from 2.94 and 3.54 km^{-1}. Half of the basins are of order 3; the others are of order 4. For each basin, mean lengths, mean areas, and mean gradients for the first three stream orders have been calculated (Table 1). Hack's law relating the drainage area above a particular point along the main stream and the along-stream distance to the divide is generally well confirmed (see, for example, basin 11 in Figure 3a). It yields an exponent α between 0.47 and 0.72 with an average value of 0.63 (Figure 3a and Table 1). These values are significantly larger than the value of 0.5 expected for random topologic network [*Rigon et al.*, 1996], as generally observed in small-scale basins [*Muller*, 1973]. Flint's law relating the main stream gradient to the drainage area also holds (Figure 3b) with an exponent β varying between 0.25 and 0.43 (Table 1). Basin shapes are variable with axial ratios ranging from 0.34 to 0.81. Hypsometric curves varies from concave upward to sigmoidal (Figures 3c and 4d) and hypsometric integrals range from 0.34 to 0.58 (Table 1).

When relief is plotted as a function of the length scale, the microscale, mesoscale, and macroscale can generally be discriminated (Figure 3d). The threshold (t_1) between the microscale and mesoscale is about 100 m for all basins. At the microscale ($l<t_1$), the relief is nearly a linear function of the length scale ($H\sim1$) (Table 1). At mesoscale the topographic roughness induces a power law dependence with H varying between 0.45 and 0.9 (Table 1). The threshold (t_2) between the mesoscale and macroscale ranges from 913 to 3427 m (Table 1) but is not always clearly defined. Therefore we have only considered the Hurst parameters related to the microscale and mesoscale domains (H_1, C_{r1} and H_2, C_{r2}, respectively) (Figure 3d).

The selected basins obey usual scaling laws and have the morphometric characteristics that are in the range of generally observed values. However, a significant variability in these properties is observed. This may reflect the fact that these basins are affected by different uplift rates and denudation rates.

5. Assessing Correlations Between Uplift Rates and Basin Morphology

5.1. Statistical Procedure (Pearson Linear Correlation Analysis)

In order to assess possible correlations between variables such as a morphometric parameter and uplift rate we performed a Pearson linear correlation analysis which is generally used in geomorphic studies [*Merritts and Vincent*, 1989; *Lifton and Chase*, 1992; *Summerfield and Hulton*, 1994]. We tested normal distribution of the variables with a Kolmogorov-Smirnov test [*Davis*, 1973] with the 5% (α=0.05) level of significance. We then determined the significance of each correlation with a Student t statistic test [*Davis*, 1973]. For each correlation the null hypothesis (H_0) was tested. H_0 states that two variables are independent (the Pearson correlation coefficient equals zero). Results were considered significant if the probability, p, to be wrong by rejecting H_0 was <5%. When this probability exceeded 5% (p>0.05), the correlation was considered nonsignificant (ns). In our analysis, with 17 data points, correlation coefficients greater than 0.48 were considered significant at the 5% significance level.

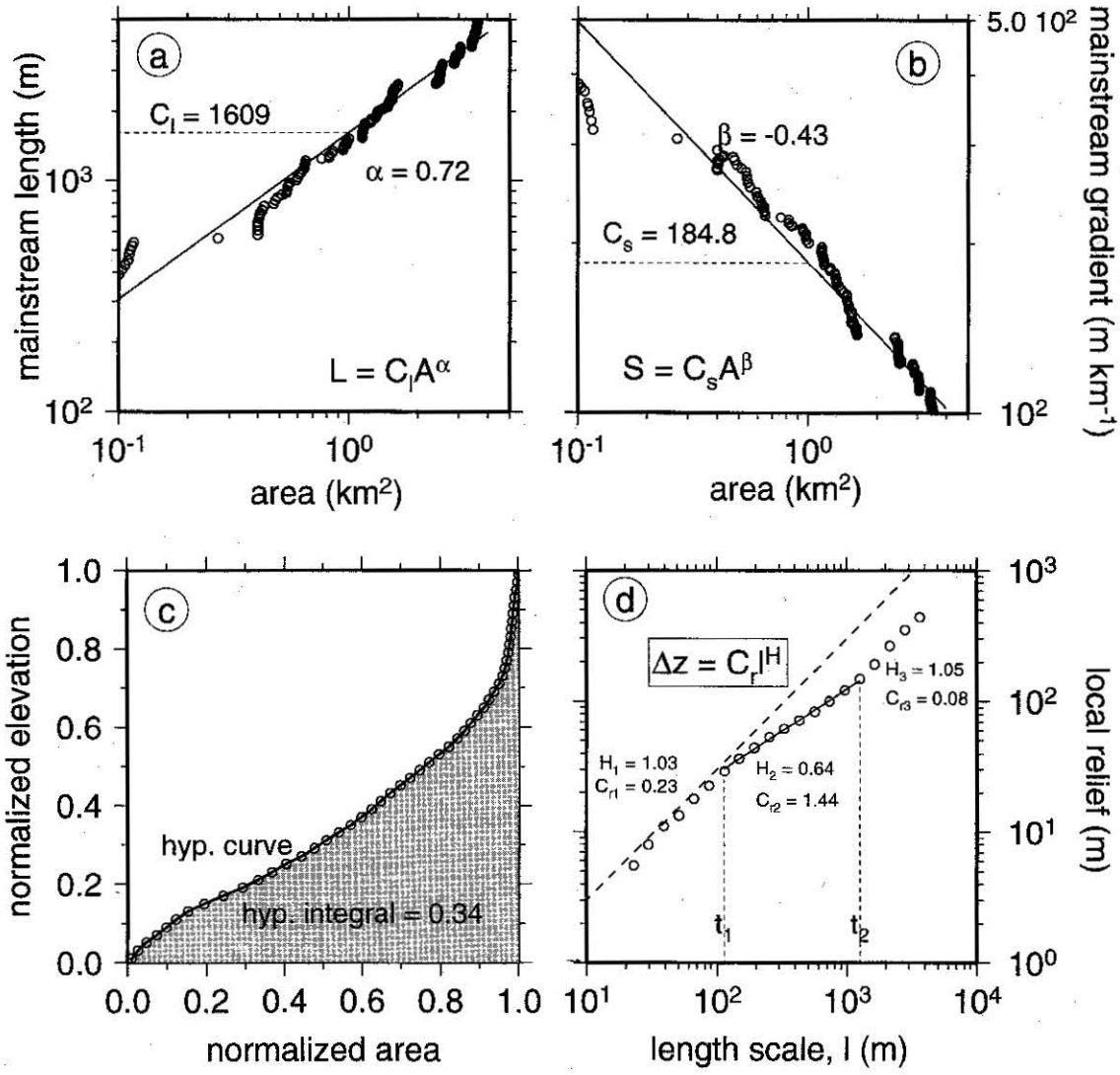

Figure 3. (a) Logarithmic plot of main stream length versus drainage area (Hack's law) for basin 15. Because precision in main stream length and drainage area decreases with decreasing area, parameters of the power law (coefficient C_l and exponent α) are determined by least squares adjustment for drainage area ranging between 10^{-1} and 3.64 km^2 (basin area). (b) Logarithmic plot of main stream gradient versus drainage area (Flint's law) for the basin 15. Because precision in main stream gradient and drainage area decreases with decreasing area, parameters of the power law (coefficient C_S and exponent β) are determined by least squares adjustment for drainage area ranging between 10^{-1} to 3.64 km^2 (basin area). (c) Hypsometric curve of basin 15 showing the proportion of the basin area under a given elevation. Elevations are normalized between 0 (elevation of the basin outlet) and 1.0 (highest point). The highest 30% of the elevation are restricted to <10% of the basin area. On the other hand, >50% of basin area lies within the lowest 30% of the elevation, which shows that a large proportion of basin area is at low elevation. Hypsometric integral, defined as the area under the hypsometric curve, is a measure of landmass in the basin. The hypsometric integral of this basin is low (0.34). (d) Logarithmic plot of mean topographic relief ($\Delta z(l)$) versus length scale (l) for the basin 15. The dashed line with a slope of 1 is shown for reference. Three domains, separated by two thresholds (t_1 and t_2), are observed. At small scale (l<100 m) the Hurst exponent is close to 1.0 (H_1=1.03). At mesoscale (100 m<l<1200 m) the relief is rougher with a Hurst exponent (H_2) of 0.64. At macroscale (l>1200 m) the local relief is nearly a linear function of the length scale (H_3=1.03). See text for discussion.

5.2. River Network

None of the morphometric parameters characterizing drainage network geometry is found to correlate to uplift rate at the 5% significance level (Table 2). The exponent of Flint's law, β, is independent of uplift rate as expected from theoretical considerations [*Willgoose*, 1994]. We also observe no correlation between the parameter C_S and uplift rate. The range of uplift rates considered in our study (6.4-15.0 mm yr^{-1}) might not be large enough to force significant variations of the coefficient C_S. An alternative explanation is that the rivers can adjust either their width or their stream gradient. Along the Bagmati and Bakeya rivers, variations of the channel width were observed to compensate for variations of tectonic uplift (Lavé and Avouac), so that the incision rate of rivers

Table 2. Pearson Linear Correlation Coefficients Between Morphometric Indices Characterizing the Channel Network, the Basin Area, and the Uplift Rate

	Hack's law		Flint's Law			Order 1			Order 2			Order 3		
	α	C_l	β	C_s	Drainage Density	Mean Length	Mean Area	Mean Gradient	Mean Length	Mean Area	Mean Gradient	Mean Length	Mean Area	Mean Gradient
Basin area	-0.16	-0.47	-0.16	-0.37	-0.14	-0.14	-0.01	-0.04	-0.01	-0.06	0.06	0.21	0.20	-0.08
Uplift rate	0.13	-0.02	0.25	0.30	0.38	0.24	-0.29	0.44	0.01	0.02	0.33	0.21	0.18	0.31

Table 3. Pearson Linear Correlation Coefficients Between Geomorphic Indices Characterizing the Drainage Basin, the Basin Area, and the Uplift Rate

						Local Relief						
						Small Scale		Mesoscale				
	Basin Area	Basin Axial Ratio	Mean Elevation	Mean Elevation - Local Base Level	Hypsometric Integral	Basin Relief	Relief Ratio	H_1	C_{r1}	H_2	C_{r2}
Basin area	1.00*	0.14	0.08	0.30	-0.11	0.45	-0.60*	0.57*	-0.49*	-0.06	-0.10
Uplift rate	-0.16	-0.15	0.68*	0.35	0.49*	-0.01	0.25	0.16	0.41	-0.16	0.45

Small scale is a few tens of meters, and mesoscale is a few hundreds of meters.
* Correlations significant at the 95% level.

could balance the tectonic uplift. Large channels can easily adjust to varying uplift rates by varying their width, but for narrow channels, variation of the stream gradients are then required (Lavé and Avouac). This may explain why we observe little correlation of the coefficient of Flint's law with tectonic uplift and why correlations between mean stream gradients and tectonic uplift increase with a decreasing order of streams (Table 2), as was also observed by *Merritts and Vincent* [1989] in California.

Our results suggest that the parameters of Hack's law (α and C_l) are independent of the uplift rate (Table 2). This is consistent with previous studies; Hack's law would probably reflect the internal organization of the channel network [*Ijjasz-Vasquez et al.*, 1993], independently of tectonic input or the ability of the river network to remove sediments.

In our data set the drainage density does not correlate significantly to the uplift rate (Table 2). This contradicts results from flume experiments [*Mosley*, 1972] and numerical modeling [*Rinaldo et al.*, 1995]. However, in our case study, the tectonic forcing may be obscured due to the influence of other forcing factors such as lithology (see *Abrahams* [1984] for a review of forcing factors on drainage density). In the study area the lithology, characterized by alternating beds of massive sandstones and more erodible mudstones, may well exert a strong control on the drainage pattern. Alternatively, one may argue that our estimate of the drainage density is biased because the channel network was extracted from the DEM on the basis of a constant area criterion [*Pilotti et al.*, 1996].

5.3. River Network

5.3.1. Basin axial ratio. In our data set the basin axial ratio is not correlated with uplift rate (r = -0.21, ns, Table 3). On the contrary, in their comparative analysis of drainage basin morphology in Taiwan, *Willemin and Knuepfer* [1994] have shown that basin axial ratio was a useful term to distinguish between different geomorphical domains, depending on their tectonic history. However, in our case the possible influence of tectonic uplift on basin axial ratio may again be obscured by some lithological control. Most of these basins are actually elongated parallel to the bedding strike (Figure 1a) with the principal stream being parallel to the bedding strike and the major tributaries perpendicular.

5.3.2. Mean elevation. Our results show a significant correlation between basin mean elevation and uplift rate (Table 3 and Figure 4a). This correlation was expected from the simple observation that the map of uplift rates (Figure 1b) closely mimics the topography (Figure 1a). This suggests that in our study area, mean elevation might be a predictor of uplift rate. Although this relation between mean elevation and uplift rate is consistent with the model of *Koons* [1989], it does not hold in all active ranges. For example, in the Southern Alps (New Zealand), uplift rate inferred from analyses of marine strandlines is the greatest at the range front where mean elevation is low [*Wellman*, 1979]. Moreover, when basin mean elevation is considered above the local base level (mean elevation minus the local base level) (Table 3), the correlation is no more significant (r=0.35, ns) (Figure 4b). This suggests that within a basin the average difference in elevation does not reflect the variations of uplift rate.

5.3.3. Hypsometric integral. In our data set we observe a systematic variation of the hypsometric curve with the uplift

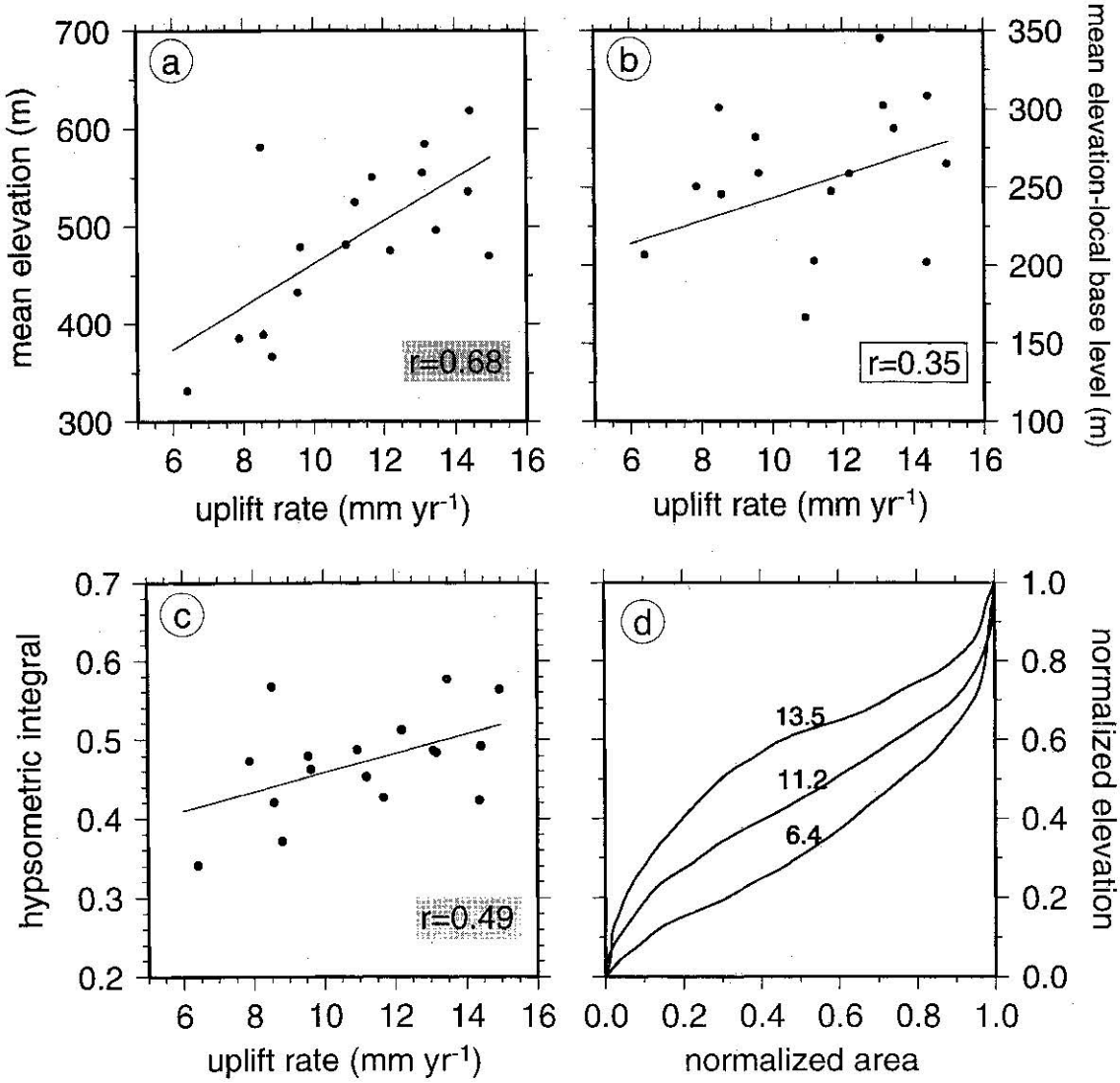

Figure 4. (a) Scatter plot of the mean elevation versus mean uplift rate for the 17 drainage basins in the study area; the solid line shows a linear fit, and r is the linear correlation coefficient. The correlation is strongly significant. This suggests that in the study area, mean elevation is a good predictor of uplift rate. (b) Scatter plot of mean elevation minus local base level versus mean uplift rate for all basins; the solid line shows a linear fit, and r is the linear correlation coefficient. The correlation is not significant. This suggests that the average difference in elevation at basin scale does not reflect the variations of uplift rate. (c) Scatter plot of the hypsometric integral versus mean uplift rate for all basins; the solid line shows a linear fit, and r is the linear correlation coefficient. The correlation is significant but moderate. This suggests that when the lithology is constant and when the tectonic pattern is simple the hypsometric integral is sensitive to uplift rate. (d) Hypsometric curves of three basins (basins 6, 8, and 15). Numeric symbols on hypsometric curves are mean uplift rates (13.5, 11.2, and 6.4 mm yr^{-1} respectively). All hypsometric curves are s-shaped. Hypsometric integrals are 0.58, 0.45, and 0.34, respectively. These hypsometric curves show an increase of the relative proportion of basin area at high elevations with uplift rate.

rate. Hypsometric curves are all s-shaped (concave upward at high elevations and concave downward at low elevations), but the relative proportion of basin area at high elevations increases with uplift rate (Figure 4d). This suggests steeper hillslope gradients where the uplift rate is higher. A similar inference was derived from the study of natural drainage basins in Japan and from simulated hypsometric curves [*Ohmori*, 1993]. This systematically induces a significant positive correlation of hypsometric integrals with uplift rates (Table 3 and Figure 4c). This result is consistent with the correlation deduced from simulated topographies by *Lifton and Chase* [1992] but contradicts their observed negative correlation in the San Gabriel Mountains, California. As pointed out by *Lifton and Chase* [1992], this difference may be due to variations of the erodibility of the rocks and the intricate tectonic pattern in the San Gabriel Mountains. Alternatively, the fact that hypsometric integral in the San Gabriel was calculated within square windows rather than real drainage basin limits may also have introduced some bias.

5.3.4. Relief. Basin relief and relief ratio are independent of uplift rate (Table 3) but are significantly correlated to basin area (r=0.45, p<0.10 and r=0.60, p<0.05, respectively). This

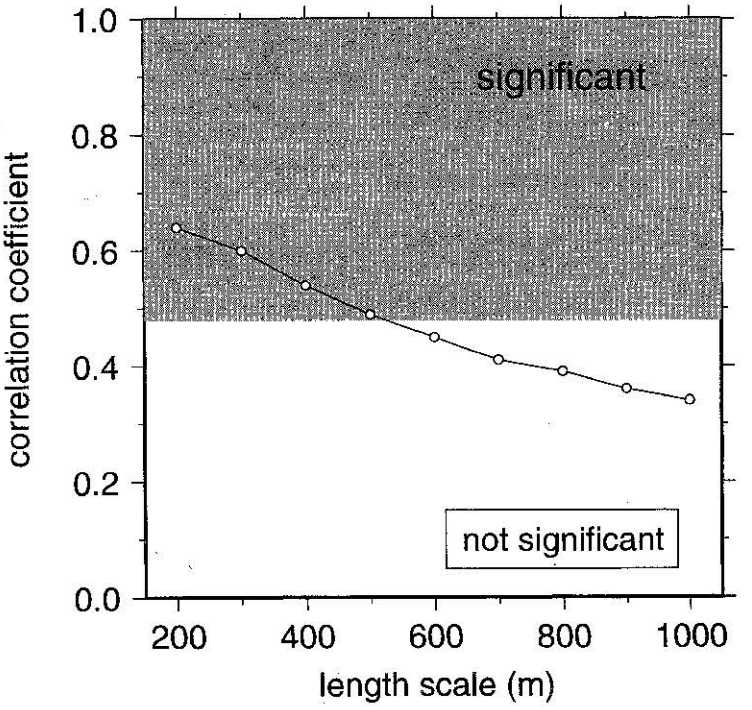

Figure 5. Correlation coefficient between uplift rate and local relief calculated at different length scales. The coefficients are only given at length scales for which the data are considered accurate (i.e., l above 200 m). Correlations are significant at short length scales (l<600 m) and are not significant at larger length scales. The local relief calculated at a few hundred meters length scale is not affected by the interpolation process used in DEM construction and is significantly correlated to the uplift rate.

last observation may explain the difference with the coastal Californian basins [*Merritts and Vincent*, 1989] in which a significant correlation with tectonic uplift was found but warns about the poor robustness of these morphometric parameters with respect to the tectonic signal. Conversely, local relief, defined as the amplitude factor C_r, correlates more strongly to uplift rate (Table 3). As also observed by *Weissel et al.* [1994], the Hurst exponent of the scaling relationship is relatively stable, and it does not correlate with uplift rate.

We have also investigated the relationship between local relief and the uplift rate at different length scales. At small length scale (l<600 m) the local relief is significantly correlated to the uplift rate, whereas the correlation vanishes at larger length scales (Figure 5). The statistical analysis suggests that the most significant correlation between uplift rate and the characteristics of the drainage basins concerns the local relief calculated at small length scales. As mentioned above, the relief at length scales shorter than 200 m may be affected by DEM flaws. Nevertheless, at larger length scales local relief is not affected by the interpolation process used in DEM construction [*Polidori et al.*, 1991] and is significantly correlated to the uplift rate. At the 200 m length scale, uplift rate is well described by the linear fit:

$$U=0.235\, r_{200} \quad (2)$$

where U is the uplift rate (mm yr^{-1}) inferred from bedding dips and r_{200} is the mean local relief calculated within the basin limit at the 200 m length scale. The correlation between local relief calculated at small length scale and uplift rate has therefore potential for predicting the uplift rate from morphological analysis of landscape. However, before doing so, the physical rationale of this correlation and, particularly, the relationship between relief and denudation rate must be investigated.

6. Discussion and Implications

6.1. Relationship Between Relief and Denudation

The significant correlation between denudation and relief is well established. From an analysis of small-scale drainage basins, *Schumm* [1963] has shown that the denudation rate increases with the basin relief. *Ahnert* [1970] suggested a significant relationship between the relief calculated at a 20 km length scale and the denudation rate for 20 basins in areas ranging from several 100 km^2 up to 100,000 km^2. More recently, *Summerfield and Hulton* [1994] have established significant correlations between the denudation rate and various variables expressing the relief (basin relief, relief ratio, mean local relief) for 33 large-scale basins exceeding 500,000 km^2. This suggests that the significant correlation between relief and denudation rate may be valid over a large range of length scales and may reflect some physical processes acting efficiently at basin scale. In the Siwaliks Hills the area for the 17 selected basins is 1 or 2 orders of magnitude smaller than that in Ahnert's study, but we have no sediment yield data to test whether or not the linear relationship between denudation and relief still holds at that range of scales. However, we have shown that relief is significantly correlated to the tectonic uplift rate and we also have evidence that denudation rate probably balances uplift rate in the study area.

6.2. Evidence for Balanced Denudation and Uplift Rates

Balanced geological sections across the fold belt indicate that it has absorbed at least 10 km of horizontal shortening (Lavé and Avouac). A simple mass balance calculation based on the geometry represented in Figure 1b inset shows that the present topography (about 720 m above the base level of 200 m elevation) represents about 5 km^2, whereas total shortening is between 60 and 90 km^2. This means that at least 90% of the material that was uplifted during fold growth has been removed by erosion. This means also that denudation rate must nearly reach tectonic uplift rate, so that the topography can be assumed to be close to a dynamic equilibrium. This is consistent with the conclusion of *Burbank and Beck* [1991], who showed such a dynamic equilibrium in the Salt range of Pakistan. However, this observation does not guarantee that at any time denudation has always balanced uplift; the observed equilibrium may actually be true only over the long term. Rivers are probably able to adapt very rapidly to climatic changes, as shown from the study of the Holocene terraces along the Bagmati and Bakeya rivers (Lavé and Avouac). Each major climatic change since the onset of the Holocene seems to have induced some short transient response no longer than about 1000 years. The present river channel of the Bagmati is characterized by a constant stream gradient and the youngest well-preserved strath terrace now 25 m above the present river was abandoned about 2.2 kyr ago. Hillslopes may, however, have a longer time response to climatic changes. Several authors have shown that the characteristic time for the landscape to adapt to climatic variations depends on the rock erodibility and may be of the order of a few tens of thousand years [*Bull*, 1991; *Tucker and Slingerland*, 1996; *Weissel and Seidl*, 1997].

Hereinafter, we consider that in the study area, present tectonic and denudation rates are equal and that the landscape, as a whole, reflects some instantaneous equilibrium between tectonic uplift, river incision, and denudation on hillslopes. This hypothesis implicitly assumes that all streams within the river network are able of incising at the rate imposed by the local uplift rate. Along the Bakeya and the Bagmati rivers, the incision rate has been shown to balance uplift rate (Lavé and Avouac). Moreover, significant correlations between relief and vertical tectonics observed at all length scales shorter than 600 m suggest that every order of the channel network is capable to adjust to the uplift rate, since the relief strongly depends on river incision. Therefore, because hillslopes processes represent the limiting process in denudation, equilibrium supposes that hillslopes can also adjust to keep balance between denudation and tectonic uplift. In the following modeling of the denudation rate, we investigate the conditions required to guarantee such an equilibrium.

6.3. Modeling the Denudation Rate

The minimum model to describe erosion processes requires the interaction between a limiting short range process for hillslopes and a long range fluvial process [*Howard et al.*, 1994]. The limit between the two processes is usually considered to be of the order of 100 m [*Dietrich and Dunne*, 1993; *Willgoose*, 1994; *Deschaux and Souriau*, 1996; *Lucazeau and Hurtrez*, 1997]. The limiting process is usually accounted for by a linear diffusion equation and the fluvial process by an advection model that states a capacity of transport proportional to runoff. In the hillslope domain, such a model does not state that efficient processes are purely diffusive processes (i.e., soil creep, rain splash, solifluction, freeze thaw, or animal induced-disturbances [*Selby*, 1993]). The diffusion equation, whose coefficient (mass diffusivity) must be calibrated, is supposed to account for the different processes efficient in the hillslope domain. The limit between hillslopes and fluvial process has been imposed at about 200 m (a contributing area of 3.84 10^{-2} km^2). In the study area the sediments produced within a basin are swept out of the channel network during monsoon time. Therefore we assume that channel networks efficiently transport the whole sediment yield to the basin outlet.

Diffusion on hillslopes is modeled using the algorithm proposed by *Beaumont et al.* [1992]. The cells are sorted from highest to lowest elevation. For each cell, we integrate the sediment flux toward the lower neighboring cells according to the law:

$$q_s = K_d \frac{l_c}{2} \frac{dz}{dx} \tag{3}$$

where q_S is the sediment flux, l_C is the cell size of the DEM, dz/dx is the slope between two adjacent cell centers, and K_d is the mass diffusivity.

The sediment flux (Q_S, in m^3 yr^{-1}) at basin outlet is defined as the cumulative sediment influx from hillslopes:

$$Q_s = \sum_k q_s^k \tag{4}$$

where k represents each cell belonging to the drainage network. The modeled denudation rate (D in m yr^{-1}) is defined as the ratio Q_S/A, where A is the basin area (m^2).

This simple model was applied on the DEM to the 17 selected basins. For each basin, the necessary mass diffusivity was estimated in order to maintain a dynamic equilibrium between uplift and denudation rates (at timescales greater than 10,000 years). Calibrated mass diffusivities range from 7.6 to 10.7 m^2 yr^{-1} (Table 4), with a mean value K_d=9.3±1.0 m^2 yr^{-1}

Table 4. Mass Diffusivity Calibrated From a Numerical Two-Process Model of Erosion

Basin	Mass Diffusivity, m^2 yr^{-1}
1	10.2
2	9.6
3	8.8
4	9.0
5	8.1
6	10.5
7	7.8
8	10.0
9	10.6
10	9.8
11	9.6
12	10.7
13	10.2
14	7.8
15	7.6
16	8.5
17	9.4

For each basin the mass diffusivity is calibrated in order to balance denudation and uplift.

(at the 1σ confidence level) in the study area. This value of mass diffusivity is several order of magnitude greater than those determined from scarps (ranging from 10^{-4} to $1.6\ 10^{-2}$ $m^2\ yr^{-1}$, see reviews by *Avouac* [1993] and *Arrowsmith et al.* [1998]). At least three nonexclusive reasons may explain this difference. (1) The high diffusivity we found may be attributed to the high erodibility of unconsolidated rocks in the Siwalik Hills and to the climatic conditions that enable rapid and efficient erosion. Particularly, the climatic effect on mass diffusivity has been evidenced at different scales. For instance, from their study of fault scarps in Idaho, *Pierce and Colman* [1986] revealed a conspicuous dependence of mass diffusivity on scarp orientation, suggesting a microclimate effect on diffusivity. At larger scale the comparison of mass diffusivities derived from scarps degradation analyses in arid, semiarid, and temperate climate regions suggests that a correlation may arise between climate and mass diffusivity [*Arrowsmith et al.*, 1998]. In New Caledonia, *Moretti and Turcotte* [1985], calculated a value of mass diffusivity of 18 $m^2\ yr^{-1}$, close to our own estimate. Emphasizing the climatic effect on diffusivity, *Moretti and Turcotte* [1985] suggested that the tropical climate affecting New Caledonia could explain such a high diffusion coefficient. (2) A second reason to explain the difference between diffusivities is that the limiting process is not diffusion at all but the incision rate itself that determines the hillslopes stability angle [*Densmore et al.*, 1998]. High mass diffusivities could reflect that nondiffusive processes, like landsliding, are the dominant mass wasting processes. From their analysis of slope distribution in several regions in northwestern Himalaya, *Burbank et al.* [1996] evidenced such a dominant role played by landsliding in landscape shaping. Studies carried out in areas with high rates of precipitation and tectonic uplift [*Kelsey*, 1980; *Pearce and Watson*, 1986; *Hovius et al.*, 1997] have also shown the dominant effect of landsliding in the erosional budget. Therefore the importance of landsliding cannot be neglected in our study area. However, the correlation between local relief and uplift rate we observed is not consistent with a dominant landsliding effect in shaping the hillslope domain. Indeed, landsliding introduces a maximum slope [*Schmidt and Montgomery*, 1995 ; *Burbank et al.*, 1996] that would destroy the correlation. The fact that landsliding would only occur on the lower part of the hillslope, as evidenced in field studies [*Megahan et al.*, 1978; *Kelsey*, 1988] and physical models [*Densmore et al.*, 1997] could account for this discrepancy. However, further field investigations are needed to test this hypothesis. (3) The fact that the difference between mass diffusivities may reflect some methodological bias cannot be excluded. As pointed out by *Moretti and Turcotte* [1985], it is difficult to compare mass diffusivity values calculated from the decay of isolated slopes with values calibrated from erosional budget integrated over an area.

6.4. Extrapolation of the Uplift Rates From Local Relief

Because the denudation process may vary with the importance of relief and also with lithologic conditions, we selected eight additional basins located in the Upper Siwalik in order to check if the linear relationship between uplift and relief still holds and could be used as a predictive tools for determining uplift rate in this specific area. These basins are cut into pebbly conglomerates that are more erodible than the sandstones of the Lower and Middle Siwaliks. The local relief for each basin at a 200 m length scale ranges from 17.2 to 26.5 m which is significantly lower than that calculated for the 17 basins in the Lower and Middle Siwaliks (Figure 6). It is likely that the importance of landsliding with respect to hillslope diffusion processes is reduced for these basin. These additional data do not show themselves the same linear trend as the previous data set. They are actually quite scattered (Figure 6), probably because the uplift rates within these basins are poorly constrained by the paucity of bedding dips and by the inaccuracy of the measurements of shallow dipping beds. However, it should be observed that the correlation established from the initial data set still holds when these eight basins are added. The linear fit is only slightly different from that found previously (equation (2)):

$$U=0.234\ r_{200} \quad (5)$$

where U is the uplift rate (mm yr^{-1}) inferred from bedding dips and r_{200} is the mean local relief calculated within the basin limit at the 200 m length scale. This suggests that the linear relationship (5) between uplift rate and local relief may then be used over the whole area to predict uplift rates (Figure 7a). According to (5) we calculated the mean uplift rate within a 1 km^2 sliding window over the whole study area.

The comparison between the map of uplift rate inferred from local relief (Figure 7a) and the map of uplift rate inferred

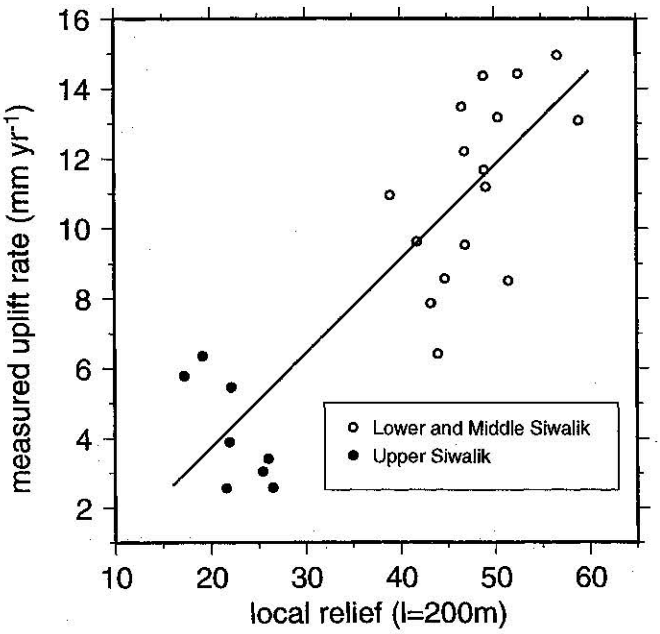

Figure 6. Scatter plot of uplift rates inferred from bedding dips versus local relief at a 200 m length scale for all basins (open circles) and for the eight basins selected in the Upper Siwalik (solid circles). The basins selected in the Upper Siwaliks do not show the same linear trend than the basins selected in the Lower and Middle Siwaliks. They are actually quite scattered probably because uplift rate is poorly constrained within Upper Siwaliks. Solid line is linear fit when the 25 basins are taken into account. This linear fit is slightly different from that found with the Lower and Middle Siwalik basins. This suggests that variations of uplift rates could dominate the variations of local relief at a 200 m length scale.

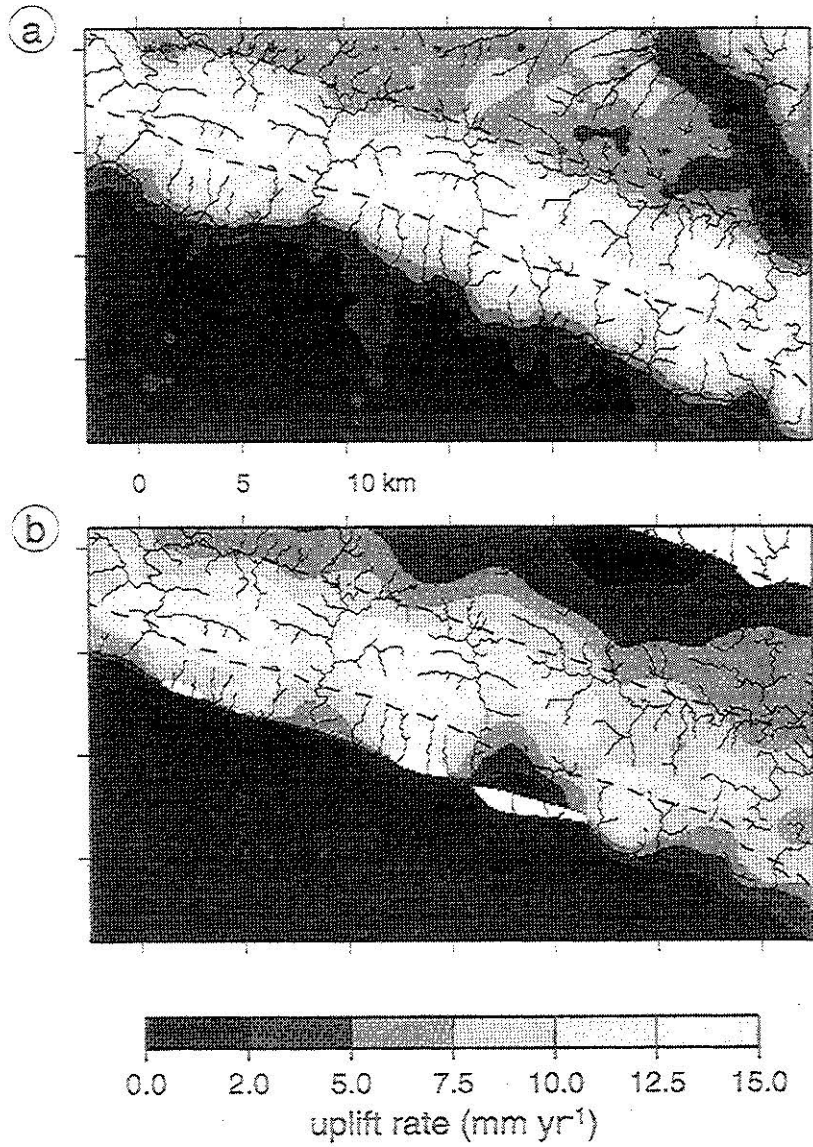

Figure 7. (a) Map of the uplift rate (or denudation rate, in case of dynamic equilibrium) inferred from the local relief at a 200 m length scale, calculated within a 1.0 km^2 moving window. (b) Map of the uplift rate inferred from bedding dips. In both cases the highest uplift rates are restricted to the axis of the anticline. This contrasts with the low elevation and low relief of the Ganges basin to the south. Within the anticline, large-scale (l=10 km) variations of uplift rate inferred from bedding dips are observed. Where uplift rate is inferred from local relief, these variations are noticeable at shorter length scale (l=5 km). North of the anticline, the uplift rate inferred from bedding dips decreases more abruptly than the uplift rate estimated from local relief. The agreement between the two independent methods to retrieve the uplift rate suggests that the variation of the tectonic uplift dominate the variations of local relief, with regard to the other forcing factors (climate, lithology, and base level). This suggests that in the Siwalik Hills uplift rate can be retrieved from topographic characteristics.

from tectonic/geometric model (Figure 7b) shows that they both present the same trend when considered at large length scales but differ in detail when considered at smaller length scales. This suggests that in our study area the local relief can be used as a predictor of uplift rate. However, inverting relief in term of uplift rates from relationship (5) in other regions is surely not possible because the relationship is highly dependent on the lithologic and climatic conditions that determine the efficiency of small-scale processes with respect to fluvial processes. Our results show that in the study area, inversion is only possible when calibration has been done. Extrapolation to other area, characterized by different tectonic, climatic, and lithologic conditions would require (1) verification that the linear relationship between local relief and uplift rate still holds and (2) site specific calibration. Comparison with other study sites would probably allow a better understanding of climatic and lithologic effects on morphological properties of landscapes.

7. Conclusions

On the basis of a cartographic knowledge of the tectonic uplift rates in a region of the Himalayan front range (Siwalik Hills), where variations of tectonic uplift are dominant over lithologic and climatic variations, an extensive number of morphometric properties have been tested in order to investigate whether or not variations of uplift rate have effects on them. In particular, in the study area we draw the following conclusions:

1. Despite high uplift rates, we have not found any correlation with the planar properties of the channel network and the drainage basins. Therefore we believe that the planar organization of drainage network obeys some laws that are independent of its ability to transport sediments. This conclusion is consistent with theoretical works on the generation of networks and with fields studies that have shown that the planar geometry is essentially related to the random propagation with little influence of deterministic processes [see *Crave and Davy*, 1997].

2. Morphometric parameters that include the vertical dimension are significantly correlated to the uplift rate, especially mean elevation, hypsometry, and relief.

3. Simple mass budgets support the hypothesis that the Siwalik Hills are in dynamic equilibrium: such an equilibrium requires that not only river incision but also hillslope processes respond at the rate of uplift on a certain timescale that could be of the order of 10^4-10^5 years.

4. A simple two-process model (linear diffusion on hillslope coupled with sediment transport in rivers) has been used to estimate the necessary mass diffusivity to guarantee the dynamic equilibrium between denudation and uplift. The calibrated value of mass diffusivity is of the order of 10 m^2 yr^{-1}. This value is several order of magnitude higher than the assumed values at small scales. This can be obtained by either a very efficient linear diffusion at small scale or by landsliding. Actually, both processes may be active given the nature of the unconsolidated rocks and the high rate of precipitation in the study area. Additional data are needed to quantify the relative importance of the different processes in landscape shaping.

5. On average, there still remains a linear correlation between uplift rate and relief that can be used for extrapolating uplift from relief in the neighboring area. However, the inversion is only valid for the lithologic and climatic conditions of the study area. It is also valid for the range of scale at which uplift rates have been estimated, that is, the order of smaller basins area (1 km^2). Given that region is exposed to extreme conditions of uplift, high precipitation, and low resistance for rocks, one can question whether the relationships between tectonic uplift and morphometric properties of landscape still hold in areas exposed to different conditions.

Appendix: Definition of Morphometric Variables

A1. Main Stream Geometry

A1.1. Hack's law. Hack's law characterizes the relationship between the topological length (measured along the stream) at a point and the upstream drainage area, along the main stream [*Rigon et al.*, 1996]

$$L=C_1 A^{\alpha} \tag{A1}$$

where L is the main stream length (m) and A is the area (km^2). In our study the parameters C_1 and α are determined by least squares adjustment (Figure 3a).

A1.2. Flint's law. Flint's law characterizes the relationship between the average slope to a point (i.e., gradient measured between the source and the current point) and the upstream drainage area, along the main stream [*Willgoose*, 1994]

$$S=C_s A^{-\beta} \tag{A2}$$

where S is the main stream mean gradient (m km^{-1}) and A is the area (km^2). In our study the parameters C_S and β are determined by least squares adjustment (Figure 3b).

A2. River Network Geometry

The drainage density is defined as the sum of channel lengths divided by the drainage area.

For a given order (according to Strahler ordering) we calculated the following parameters:

1. The mean length is defined as the average value of the topological length (length calculated along the stream) of the streams.

2. The mean area is the average value of the area draining through the outlet of the subbasins.

3. The mean gradient is defined as the average value of the difference in elevation between the source and the outlet divided by the topological length.

A3. Characterization of the Drainage Basin

A3.1. Basin axial ratio. The aspect ratio is a measure of the basin planform. This index is defined as the ratio of the short axis to the long axis of the equivalent ellipse of the basin [*Moussa*, 1991]). For an elongated basin the basin aspect ratio is close to 0, and for a subcircular-shaped basin the ratio is close to 1. Each basin is a planar surface, represented by n cells in a mesh, with x-y coordinates.

The coordinates of the gravity center of the basin are given by

$$x_g=\frac{\sum x_i}{n}, \qquad y_g=\frac{\sum y_i}{n} \tag{A3}$$

Variances and covariance are

$$\mathrm{Var}_x=\frac{n\sum x_i^2-(\sum x_i)^2}{n(n-1)}, \quad \mathrm{Var}_y=\frac{n\sum y_i^2-(\sum y_i)^2}{n(n-1)}, \quad \mathrm{Cov}_{xy}=\frac{n\sum x_i\times y_i-(\sum x_i\times\sum y_i)}{n(n-1)} \tag{A4}$$

Principal axes of the moment of inertia are given by

$$I_{\min}^{\max}=\frac{\mathrm{Var}_x+\mathrm{Var}_y}{2}\pm\sqrt{\left(\frac{\mathrm{Var}_x-\mathrm{Var}_y}{2}\right)^2+\mathrm{Cov}_{xy}^2} \tag{A5}$$

$$I_{\min}=\frac{\pi ab^3}{4} \quad \text{and} \quad I_{max}=\frac{\pi a^3 b}{4} \tag{A6}$$

where a and b are the half-long and the half-short axis of the equivalent ellipse of the basin.

The basin axial ratio is given by

$$\frac{b}{a} = \sqrt{\frac{I_{min}}{I_{max}}} \quad \text{(A7)}$$

A3.2. Mean elevation and local base level elevation. For each basin the mean elevation is estimated as the zonal average value of the elevations. We have also determined the elevation of the local base level (along one the four main rivers that cross the anticline) in order to calculate the mean elevation above local base level.

A3.3. Hypsometric curve and hypsometric integral. The hypsometric curve (Figure 3c) represents the relative proportion of a basin area that lies below a given elevation. Elevations and basin area are normalized between 0 and 1.0.

The hypsometric integral represents the area under the hypsometric curve.

We consider a basin represented by N cells in a mesh. Elevations are normalized between 0 and 1.0:

$$\text{alt}_{\text{norm}} = \frac{\text{alt} - \text{alt min}}{\text{alt max} - \text{alt min}} \quad \text{(A8)}$$

where alt is the elevation of one cell, and altmin and altmax are the minimum and the maximum elevations within the basin, respectively.

Below a given elevation, alt, the proportion of basin area is

$$\frac{\sum_i H(\text{alt} - \text{alt}_i)}{N} \quad \text{(A9)}$$

where $H(x)$ is the Heaviside unit step function:

$$H(x) = \begin{cases} 0, x < 0 \\ 1, x > 0 \end{cases} \quad \text{(A10)}$$

The hypsometric integral is

$$\text{Int} = \frac{1}{N} \int_{\text{alt min}}^{\text{alt max}} \sum_i H(\text{alt} - \text{alt}_i) \quad \text{(A11)}$$

$$\text{Int} = \frac{1}{N}\left[N(\text{alt max} - \text{alt min}) - \left(N \times \text{at max} - \sum_i \text{alt}_i \right) \right] \quad \text{(A12)}$$

$$\text{Int} = \left(\overline{\text{alt}} - \text{alt min} \right) \quad \text{(A13)}$$

where $\overline{\text{alt}}$ is mean elevation within basin limit.

The normalization leads to

$$\text{Int} = \frac{\overline{\text{alt}} - \text{alt min}}{\text{alt max} - \text{alt min}} \quad \text{(A14)}$$

The hypsometric integral is a measure of the landmass in the basin. A low value indicates that a large proportion of the basin is at low elevation while a high value indicates that a large proportion of the basin is at high elevation.

A3.4. Basin relief. For drainage basins of similar size the basin relief is the elevation difference between the highest and the lowest point in the drainage basin [*Ohmori*, 1993].

A3.5. Relief ratio. The relief ratio is the basin relief normalized by the length of the basin [*Summerfield and Hulton*, 1994]. The length of the basin is given by the long axis of the equivalent ellipse of the basin.

A3.6. Local relief. The mean local relief is defined by the following equation [*Weissel et al.*, 1994]

$$\Delta z(l) = \left\langle \left| z(x+l) - z(x) \right| \right\rangle \quad \text{(A15)}$$

where Δz is the local relief, z is the elevation, and l is the length scale. The angle brackets denote spatial averaging. Local relief can be expressed as a power function of the length scale [*Weissel et al.*, 1994]

$$\Delta z(l) = C_r l^H \quad \text{(A16)}$$

where C_r is a coefficient independent on l and H is the Hurst exponent.

Acknowledgments. We thank P. Knuepfer, A. Densmore, and M. Ellis for constructive and thorough reviews. We are very grateful to S. Hurtrez-Boussès and Ben Holtzman for helpful discussions, R. Moussa and M-G. Tournoud for providing their software "MAD" to extract the channel network from DEM, and A. Delplancke for help with drawings. Financial support was provided by the Ministère de l'Education Nationale, de l'Enseignement Supérieur et de la Recherche (AMN, Université Montpellier II, France) for one of us (J.-E. H.) and by the CNRS-INSU research programs "DBT 2 Dynamique des fleuves et érosion" and "PROSE".

References

Abrahams, A.D., Channel networks: A geomorphological perspective, *Water Resour. Res.*, *20*, 161-187, 1984.

Ahnert, F., Functional relationships between denudation, relief and uplift in mid-latitude drainage basin, *Am. J. Sci.*, *268*, 243-263, 1970.

Ahnert, F., Local relief and the height limits of mountain ranges, *Am. J. Sci.*, *284*, 1035-1055, 1984.

Apple, E., W. Rösler, and G. Corvinus, Magnetostratigraphy of the Miocene-Pleistocene Surai khola Siwaliks West Nepal, *Geophys J. Int.*, *105*, 191-198, 1991.

Armijo, R., B. Meyer, G.C.P. King, A. Rigo, and D. Papanastassiou, Quaternary evolution of the Corinth rift and its implications for the late Cenozoic evolution of the Aegean, *Geophys. J. Int.*, *126*, 11-53, 1996.

Arrowsmith, J.R., D.D. Pollard, and D.D. Rhodes, Hillslope development in areas of active tectonics, *J. Geophys. Res.*, *101*, 6255-6275, 1996.

Arrowsmith, J.R., D.D. Rhodes, and D.D. Pollard, Morphologic dating of scarps formed by repeated slip events along the San Andreas Fault, Carrizo Plain, California, *J. Geophys. Res.*, *103*, 10141-10160, 1998.

Avouac, J.P., Analysis of scarp profiles: evaluation of errors in morphologic dating, *J. Geophys. Res.*, *98*, 6745-6754, 1993.

Band, L.E., Topographic partition of watersheds with digital elevation models, *Water Resour. Res.*, *22*, 15-24, 1986.

Beaumont, C., P. Fullsack, and J. Hamilton, Erosional control of active compressional orogens, in *Thrust Tectonics*, edited by K.R.McClay, pp. 1-18, Chapman and Hall, New York, 1992.

Begin, Z.B., D.F. Meyer, and S.A. Schumm, Development of longitudinal profiles of alluvial channels in response to baselevel lowering, *Earth Surf. Processes Landforms*, *6*, 49-68, 1981.

Bull, W.B., *Geomorphic Response to Climatic Change*, 326 pp., Oxford Univ. Press, New York, 1991.

Bull, W.B., and P.L.K. Knuepfer, Streams adjustments to uplift and climatic changes, Charwell River, New Zealand, *Geomorphology*, *1*, 15-32, 1987.

Burbank, D.W., and R.A. Beck, Rapid long-term rates of denudation, *Geology*, *19*, 1169-1172, 1991.

Burbank, D.W., J. Leland, E. Fielding, R.S. Anderson, N. Brozovic,

M.R. Reid, and C. Duncan, Bedrock incision, rock uplift and threshold hillslopes in the northwestern Himalayas, *Nature*, *379*, 505-510, 1996.

Chase, C.G., Fluvial landsculpting and the fractal dimension of topography, *Geomorphology*, *5*, 39-57, 1992.

Crave, A., and P. Davy, Scaling relationships of channel networks at large scales: Examples from two large-magnitude watersheds in Brittany, France, *Tectonophysics*, *269*, 91-111, 1997.

Davis, J.C., *Statistics and Data Analysis in Geology*, 550 pp., John Wiley, New York, 1973.

Delcaillau, B., G. Herail, T. Mascle, and G. Mascle, Evolution géomorphostructurale de fronts de chevauchements actifs: Le cas des chevauchements intrasiwaliks du Népal central, *Z. Geomorphol.*, *31*, 339-360, 1987.

Densmore, A.L., R.S. Anderson, B.G. McAdoo, and M.A. Ellis, Hillslope evolution by bedrock landslides, *Science*, *275*, 369-372, 1997.

Densmore, A.L., M.A. Ellis, and R.S. Anderson, Landsliding and the evolution of normal-fault-bounded mountains, *J. Geophys. Res.*, *103*, 15203-15219, 1998.

Deschaux, V., and M. Souriau, Topography of large-scale watersheds: fractal texture and global drift. Application to the Mississippi basin, *Earth Planet. Sci. Lett.*, *143*, 257-267, 1996.

Dietrich, W.E., and T. Dunne, The channel head, in *Channel Network Hydrology*, edited by K. Beven, and M.J. Kirkby, pp. 175-219, John Wiley, New York, 1993.

Harrison, T.M., P. Copeland, S.A. Hall, J. Quade, S. Burner, T.P. Ojha, and W.S.F. Kidd, Isotopic preservation of Himalayan/Tibetan uplfit, denudation and climatic histories of two molasse deposits, *J. Geol.*, *101*, 157-175, 1993.

Hovius, N., Regular spacing of drainage outlets from linear mountain belts, *Basin Res.*, *8*, 29-44, 1996.

Hovius, N., C.P. Stark, and P.A. Allen, Sediment flux from a mountain belt derived by landslide mapping, *Geology*, *25*, 231-234, 1997.

Howard, A.D., W.E. Dietrich, and M.A. Seidl, Modeling fluvial erosion on regional to continental scales, *J. Geophys. Res.*, *99*, 13971-13986, 1994.

Ijjasz-Vasquez, E.J., R.L. Bras, and R. Rodriguez-Iturbe, Hack's relation and optimal channel networks: The elongation of river basins as a consequence of energy minimization, *Geophys. Res. Lett.*, *20*, 1583-1586, 1993.

Keller, E.A., Investigation of active tectonics: use of surficial Earth processes, in *Active Tectonics*, edited by R.E. Wallace, pp. 136-147, Natl. Acad. Press, Washington, D. C., 1986.

Kelsey, H.M., A sediment budget and an analysis of sediment processes in the Van Duzen River basin, north coastal California, 1941-1975, *Geol. Soc. Am. Bull.*, *91*, 1119-1216, 1980.

Kelsey, H.M., Formation of inner gorges, *Catena*, *15*, 433-458, 1988.

Koons, P.O., The topographic evolution of collisional mountain belts: A numerical look at the Southern Alps, New Zealand, *Am. J. Sci.*, *289*, 1041-1069, 1989.

Lajoie, K.R., Coastal tectonics, in *Active Tectonics*, edited by R.E. Wallace, pp. 95-124, Natl. Acad. Press, Washington, D.C., 1986.

Lavé, J., Tectonique et érosion: L'apport de la dynamique fluviale à l'étude sismotectonique de l'Himalaya du Népal central, thèse, Univ. Paris VII, Paris, 1997.

Lifton, N.A., and C.G. Chase, Tectonic, climatic and lithologic influences on landscape fractal dimension and hypsometry: implications for landscape evolution in the San Gabriel Mountains, California, *Geomorphology*, *5*, 77-114, 1992.

Lucazeau, F., and J.E. Hurtrez, Length scale dependence of relief along the southeastern border of Massif Central (France), *Geophys. Res. Lett.*, *24*, 1823-1826, 1997.

Lyon-Caen, H., and P. Molnar, Constraints on the structure of the Himalaya from an analysis of gravity anomalies and a flexural model of the lithosphere, *J. Geophys. Res.*, *88*, 8171-8191, 1983.

Mayer, L., Tectonic geomorphology of escarpments and mountain fronts, in *Active Tectonics*, edited by R.E. Wallace, pp. 125-135, Natl. Acad. Press, Washington, D.C., 1986.

Medlicot, H.B., On the geological structure and relation of the southern portion of the Himalayan range between river Ganga and Ravee. *Mem. Geol. Surv. India*, *3*, 1964.

Megahan, W.F., N.F. Day, and T.M. Bliss, Landslide occurrence in the western and central Northern Rocky Mountain physiographic province in Idaho, in *Forest Soils and Land Use: Proceedings of the Fifth North American Forest Soils Conference*, edited by C.T. Youngberg, pp. 116-139, Colo. State. Univ., Fort Collins, 1978.

Merritts, D., and K.R. Vincent, Geomorphic response of coastal streams to low, intermediate, and high rates of uplift, Mendocino triple junction region, northern California, *Geol. Soc. Am. Bull.*, *101*, 1373-1388, 1989.

Merritts, D.J., K.R. Vincent, and E.E. Wohl, Long river profiles, tectonism, and eustasy: A guide to interpreting fluvial terraces, *J. Geophys. Res.*, *99*, 14031-14050, 1994.

Mizutani, T., Longitudinal profile evolution of valleys on coastal terraces under the compound influence of eustasy, tectonism and marine erosion, *Geomorphology*, *17*, 317-322, 1996.

Montgomery, D.R., and W.E. Dietrich, Source areas, drainage density and channel initiation, *Water Resour. Res.*, *25*, 1907-1918, 1989.

Moretti, I., and D.L. Turcotte, A model for erosion, sedimentation, and flexure with application to New Caledonia, *J. Geodyn.*, *3*, 155-168, 1985.

Mosley, M.P., An experimental study of rill erosion, M.S. thesis, Colo. State Univ., Fort Collins, 1972.

Moussa, R., Variation spatio-temporelle et modélisation hydrologique. Application au bassin du Gardon d'Anduze, thèse, Univ. Montpellier II, Montpellier, France, 1991.

Moussa, R., M.-G. Tournoud, and C. Bocquillon, Extraction and analysis of the structure of drainage network from digital elevation models, in *Computer Methods and Water Resources*, pp.14, Byblos, Lebanon, 1997.

Muller, J.E., Re-evaluation of the relationship of master streams and drainage basins, *Geol. Soc. Am. Bull.*, *84*, 3127-3130, 1973.

Nakata, T., Active faults of the Himalaya of India and Nepal, *Spec. Pap. Geol. Soc. Am.*, *232*, 243-264, 1989.

Ohmori, H., Changes in the hypsometric curve through mountain building resulting from concurrent tectonics and denudation, *Geomorphology*, *8*, 263-277, 1993.

Pearce A.J., and A.J. Watson, Effects of earthquake-induced landslides on sediment budget and transport over 50-yr period, *Geology*, *14*, 52-55, 1986.

Pierce, K.L., and S.M. Colman, Effect of height and orientation (microclimate) on geomorphic degradation rates and processes, late-glacial terrace scarps in central Idaho, *Geol. Soc. Am. Bull.*, *97*, 869-885, 1986.

Pilotti, M., C. Gandolfi, and G.B. Bischetti, Identification and analysis of natural channel networks from digital elevation models, *Earth Surf. Processes Landforms*, *21*, 1007-1020, 1996.

Polidori, L., J. Chorowicz, and R. Guillande, Description of terrain as a fractal surface and application to digital elevation model quality assessment, *Photogramm. Eng. Remote Sens.*, *57*, 1329-1332, 1991.

Press, W.H., B.P. Flannery, S.A. Teukolsky, and W.T. Vetterling, *Numerical Recipes*, Cambridge Univ. Press, New York, 1989.

Rigon, R., I. Rodriguez-Iturbe, A. Maritan, A. Giacometti, D.G. Tarboton, and A. Rinaldo, On Hack's law, *Water Resour. Res.*, *32*, 3367-3374, 1996.

Rinaldo, A., W.E. Dietrich, R. Rigon, G.K. Vogel, and I. Rodriguez-Iturbe, Geomorphological signatures of varying climate, *Nature*, *374*, 632-635, 1995.

Rockwell, T.K., E.A. Keller, M.N. Clark, and D.L. Johnson, Chronology and rates of faulting of Ventura river terraces, California, *Geol. Soc. Am. Bull.*, *95*, 1466-1474, 1984.

Schelling, D., and K. Arita, Thrust tectonics, crustal shortening, and the structure of the far-eastern Nepal Himalaya, *Tectonics*, *10*, 851-862, 1991.

Schmidt, K.M., and D.R. Montgomery, Limits to relief, *Science*, *270*, 617-620, 1995.

Schumm, S.A., The disparity between present rates of denudation and orogeny, *U.S. Geol. Surv. Prof. Pap.*, *454 (H)*, 1-13, 1963.

Schumm, S.A., Alluvial river response to active tectonics, in *Active Tectonics*, edited by R.E. Wallace, pp. 80-94, Natl. Acad. Press, Washington, D.C., 1986.

Seeber, L., J. Armbruster, and R. Quittmeyer, Seismicity and continental subduction in the Himalayan arc, in *Zagros, Hindu Kush, Himalaya, Geodynamic Evolution*, Geodyn. Ser., vol. 3, edited by H.K. Gupta and F.M. Delany, pp. 215-242, AGU, Washington, D.C., 1981.

Selby, M.J., *Hillslope Materials and Processes*, Oxford Univ. Press, New York, 1993.

Strahler, A.N., Dynamic basis of geomorphology, *Geol. Soc. Am. Bull.*, *63*, 923-938, 1952a.

Strahler, A.N., Hypsometric (area-altitude) analysis of erosional topography, *Geol. Soc. Am. Bull.*, *63*, 1117-1141, 1952b.

Summerfield, M.A., Sub-aerial denudation of passive margins: Regional elevation versus local relief models, *Earth Planet. Sci. Lett.*, *102*, 406-469, 1991.

Summerfield, M.A., and N.J. Hulton, Natural controls of fluvial denudation rates in major world drainage basins, *J. Geophys. Res.*, *99*, 13871-13883, 1994.

Suppe, J., Geometry and kinematics of fault-bend folding, *Am. J. Sci.*, *283*, 684-721, 1983.

Tucker, G.E., and R. Slingerland, Predicting sediment flux from fold and thrust belts, *Basin Res.*, *8*, 329-349, 1996.

Turcotte, D.L., Geomorphology, in *Fractals and Chaos in Geology and Geophysics*, pp. 95-102, Cambridge Univ. Press, New York, 1992.

Vergne, M., and M. Souriau, Quantifying the transition beween tectonic trend and mesoscale texture in topographic data, *Geophys. Res. Lett.*, *20*, 2139-2141, 1993.

Weissel, J.K., and M.A. Seidl, Influence of rock strength properties on escarpment retreat across passive continental margins, *Geology*, 631-634, 1997.

Weissel, J.K., L.F. Pratson, and A. Malinverno, The length-scaling properties of topography, *J. Geophys. Res.*, *99*, 13997-14012, 1994.

Wellman, H.W., An uplift map for the South Island of New Zealand, and a model for uplift of the Southern Alps, *Bull. R. Soc. N. Z.*, *18*, 13-21, 1979.

Willemin, J.H., and P.L.K. Knuepfer, Kinematics of arc-continent collision in the eastern Central Range of Taiwan inferred from geomorphic analysis, *J. Geophys. Res.*, *99*, 20267-20280, 1994.

Willgoose, G., A statistic for testing the elevation characteristics of landscape simulation models, *J. Geophys. Res.*, *99*, 13987-13996, 1994.

J.-P. Avouac, Laboratoire de Géophysique, CEA, BP 12, F-91680 Bruyères-le-Chatel, France. (avouac@ldg.bruyeres.cea.fr)

J.-E. Hurtrez, Laboratoire de Géologie, UMR 8538 CNRS Ecole Normale Supérieure, 24, rue Lhomond, F-75231 Paris, France. (hurtrez@geologie.ens.fr)

J. Lavé, Laboratoire de Géodynamique des Chaînes Alpines, UPRES A 5025 CNRS Université Joseph Fourier Université de Savoie, 15, Rue Maurice Gignoux, F-38031 Grenoble, France.

F. Lucazeau, Laboratoire de Géophysique et Tectonique, UMR 5573 CNRS Université de Montpellier II, F-34095 Montpellier, France. (francis@dstu.univ-montp2.fr)

(Received January 20, 1998; revised November 12, 1998; accepted November 20, 1998.)